Supporting information available for

Synthesis of Pyridine-Functionalized Cyclic Aromatic Triamide and Formation of Copper Coordination Polymeric Complexes

Koji Takagi,[*a] Taiga Shirai,[a] Daiki Miyamoto,[a] Takuya Nakashima,[b] Tomoyuki Ikai,[c,d] Yutaka Ie[e] and Takanori Fukushima[f]

[a] Graduate School of Engineering, Nagoya Institute of Technology, Gokiso-cho, Showa-ku, Nagoya 466-8555, Japan
[b] Graduate School of Science, Osaka Metropolitan University, 3-3-138 Sugimoto, Sumiyoshi-ku, Osaka 558-8585, Japan
[c] Graduate School of Engineering, Nagoya University, Furo-cho, Chikusa-ku, Nagoya, Aichi 464-8603, Japan
[d] Precursory Research for Embryonic Science and Technology (PRESTO), Japan Science and Technology Agency (JST), Kawaguchi, Saitama 332-0012, Japan
[e] The Institute of Scientific and Industrial Research (SANKEN), Osaka University, 8-1 Mihogaoka, Ibaraki, Osaka 567-0047, Japan
[f] Laboratory for Chemistry and Life Science, Institute of Integrated Research, Institute of Science Tokyo, 4259 Nagatsuta, Midori-ku, Yokohama 226-8501, Japan

Contents

S1. General
S2. Synthesis of Compounds
S3. HPLC Chromatograms
S4. Spectral Data
S5. XRD data
S6. Theoretical Calculations
S7. References

S1. General

Materials

All materials were obtained from commercial suppliers and used without purification unless otherwise noted. Anhydrous tetrahydrofuran (THF) and dichloromethane (DCM) were purchased from Kanto Chemical Co. Other solvents were dried and distilled following to standard methods, and stored under nitrogen atmosphere. Cyclic aromatic triamide **C3A-2Br** for introducing pyridine unit was synthesized following our reported procedure.[S1]

Instruments

Purifications

A Yamazen flash chromatographic system AI-580S was used for the purification using Hi-Flash columns. The purifications with preparative gel permeation chromatography (GPC) were carried out on a Japan analytical industry LC-9210 system using tandem JAIGEL 1H, 2H, and 2.5H columns ($CHCl_3$ as an eluent, flow rate = 3.8 mL/min) equipped with a UV detector monitored at 254 nm. The chromatographic separations of enantiomers were performed using a flash chromatographic system AI-580S equipped with DAICEL CHIRALFLASH IC as a chiral stationary phase (CSP) column.

Characterizations

The high resolution electrospray ionization mass spectra (HR ESI-MS) were obtained on a Waters Synapt G2 HDMS. The solution-state nuclear magnetic resonance (NMR) spectra were obtained on a Bruker Ascend™400 FT-NMR spectrometer using tetramethylsilane (^{1}H NMR) and solvent residual peaks (^{13}C NMR) as the internal standard. The solid-state magic angle spinning (MAS) ^{31}P NMR spectra were obtained on a JEOL JNM-ECZ600II FT-NMR spectrometer using 3.2 mm HXMAS probe and 3.2 mm zirconia sample tube. The rotation speed was 20 kHz, and the chemical shift was calibrated based on 1.0 ppm $NH_4H_2PO_4$ as the secondary external standard. The elemental analyses (EA) were performed on an Elementar vario EL cube. X-ray photoelectron spectroscopy (XPS) was performed on a ULVAC-PHI 5000 Versa Probe III equipped with a monochromatic 11-426 E-beam scanning X-ray source (Al Kα). The data was calibrated to the peaks at 284.80 eV for C 1s. X-ray diffraction (XRD) measurements were performed using an FR-E X-ray diffractometer equipped with a two-dimensional R-axis IV detector (Rigaku) involving an imaging plate (Fujifilm). A collimated X-ray beam (Cu Kα = 0.154 nm, 0.3 mm) was used, with a camera length was set to 300 mm. The beam was directed through powder samples enclosed in a soda glass capillary tube (ϕ = 1.0 mm, thickness = 0.01 mm) at 25 °C. The exposure time for each measurement was set to 5 min.

Spectroscopic analyses in solution state

The ultraviolet (UV) absorption and photoluminescence (PL) spectra were recorded on a Shimadzu UV-2600I spectrophotometer and RF-5300 spectrofluorometer, respectively, using a 10 mm quartz cell. The fluorescence quantum yields were determined relative to quinine sulfate ($\Phi = 0.55$) as a standard. The absorption and circular dichroism (CD) spectra were obtained in a 10 mm quartz cell using a JASCO V-750 spectrophotometer and a JASCO J-1500 spectropolarimeter, respectively. The temperature was controlled with a JASCO ETCS-900 apparatus. The circularly polarized luminescence (CPL) spectra were recorded at 25 °C on a JASCO CPL-300 spectrophotometer with a 10 mm quartz cell. A scanning rate of 200 nm/min, an excitation slit width of 3000 μm, a monitoring slit width of 3000 μm, a response time of 2 seconds, and 4 times accumulations were employed for the CPL measurements.

Spectroscopic analyses in powder state

The UV absorption spectra were recorded on a Shimadzu UV-2600I spectrophotometer using an integrating sphere attachment and a powder sample holder. The PL spectra of powder samples were measured with an Olympus BX-51 polarizing microscope connected to a Hamamatsu PMA-11 photodetector (< 800 nm) through an optical fiber. Excitation to the powder was performed with a high-pressure mercury lamp through a band path filter (330-385 nm) and the emission band was collected through a long path filter (>420 nm). The PL spectra were also recorded on a Hamamatsu Quantaurus-QY Plus C13534 instrument and absolute QYs were obtained with an integrating sphere C11347. The CPL spectra were recorded in the same instruments as in the solution state. The ground solid samples, placed between two quartz plates, were used for the powder-state CPL measurements. The measurement conditions were the same as those used for the solution measurements except for the accumulation times (16 times).

Emission kinetics

The fluorescence lifetime measurement was carried out with a DeltaFlex (HORIBA) time-correlated single-photon-counting (TCSPC) instrument with a 367 nm LED (SpectraLED-370) as an excitation light source. The intensity-weighted average lifetimes (τ) were used to determine the radiative and nonradiative rate constants of the exponential decay components using the following equation, where τ_i are the lifetimes and A_i are the pre-exponential factors.

$$\tau = \frac{\sum A_i {\tau_i}^2}{\sum A_i \tau_i}$$

S2. Synthesis of Compounds

C3A-1EPy

A mixture of **C3A-2Br**[S1] (200 mg, 0.24 mmol), 4-[2-(tributylstannyl)ethynyl]pyridine (500 mg, 1.28 mmol), and $Pd(PPh_3)_4$ (45.2 mg, 39 μmol) in toluene (30 mL) was heated to reflux overnight. After toluene was removed, residue was extracted with CH_2Cl_2 and washed with saturated NH_4Cl solution, dried over $MgSO_4$, and evaporated to dryness. The crude product was purified by preparative GPC ($CHCl_3$) and SiO_2 column chromatography (hexane : ethyl acetate = 2:1, Rf = 0.31) to obtain **C3A-1EPy** as pale yellow solid in 166 mg (79% yield). ^{1}H NMR (400 MHz, CHLOROFORM-*d*) δ ppm 0.85 (m, 9H), 1.22 (m, 30H), 1.58 (m, 6H), 3.51 (m, 1H), 3.68 (m, 1H), 3.84 (t, J=7.6 Hz, 2H), 4.07 (m, 1H), 6.69 (dd, J = 8.2 Hz, 2.4 Hz, 1H), 6.82 (dd, J = 8.2 Hz, 2.0 Hz, 1H), 6.93 (dt, J = 8.2 Hz, 2.4 Hz, 1H), 6.97 (dd, J = 8.1 Hz, 1.9 Hz, 1H), 7.12 (dd, J = 8.2 Hz, 2.0 Hz, 1H), 7.19 (m, 3H), 7.32 (dd, J = 8.2 Hz, 1.9 Hz, 1H), 7.42 (dd, J = 4.4 Hz, 1.6 Hz, 2H), 7.46 (dd, J = 4.4 Hz, 1.6 Hz, 2H), 8.69 (m, 4H). ^{13}C NMR (100 MHz, CHLOROFORM-*d*) δ ppm 14.1, 22.6, 26.8, 26.9, 27.0, 27.6, 27.7, 27.8, 29.1, 29.2, 29.3, 31.7, 49.0, 49.1, 89.1, 89.8, 93.1, 94.7, 120.8, 123.4, 125.5, 127.2, 127.6, 127.8, 128.1, 128.6, 128.8, 129.3, 130.0, 131.5, 133.5, 135.0, 136.9, 139.8, 141.5, 143.7, 144.9, 150.1, 150.2, 167.4, 170.4, 170.9. HR ESI-MS (m/z) calcd for **C3A-1EPy**+H^+: 896.5479, found: 896.5480.

C3A-CuP A

C3A-1EPy (9.0 mg, 0.01 mmol) was added to an CH_3CN solution (0.5 mL) of CuI (3.8 mg, 0.02 mmol) in a sample vial, and the mixture was stirred at room temperature for 3 h. The precipitate was filtered and washed with CH_3CN and dried under vacuum to obtain a yellow solid in 9.4 mg (73%).

Elemental analysis calcd for $C_{59}H_{69}Cu_2I_2N_5O_3$: C 55.49, H 5.45, N 5.48, ; found: C 54.92, H 5.56, N 5.48.

C3A-CuP B

C3A-1EPy (9.0 mg, 0.01 mmol) was added to an anhydrous THF solution (1.5 mL) of $Cu_2I_2(PPh_3)_3$ (12 mg, 0.01 mmol) in a sample vial, and the mixture was stirred at room temperature for 3 h. The product was purified by precipitating in hexane three times and dried under vacuum to obtain an orange solid in 14 mg (66%).

Elemental analysis calcd for $C_{95}H_{99}Cu_2I_2N_5O_3P_2$: C 63.33, H 5.54, N 3.89, ; found: C 61.35, H 5.46, N 3.26.

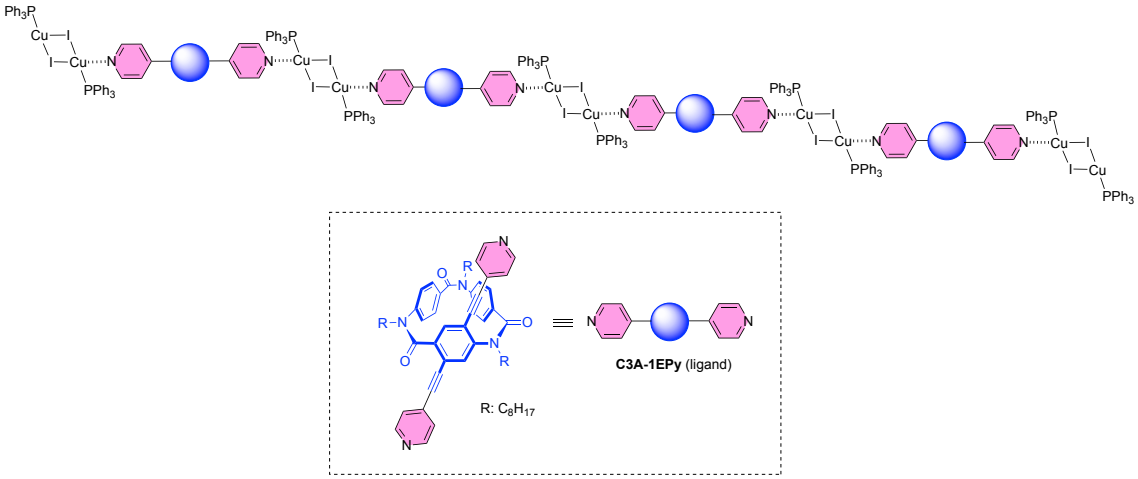

Scheme S1. Plausible chemical structure of **C3A-CuP B** estimated by elemental analysis.

S3. HPLC Chromatograms

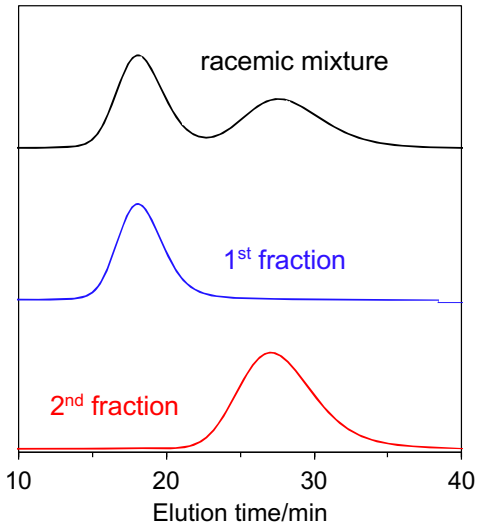

Figure S1. HPLC chromatograms of **C3A-1EPy** on a DAICEL CHIRALPAK IC column (4.6 mm (i.d.)×100 mm, 20 μm) with DCM/EtOH/DEA (99/1/0.1 in volume ratio) as an eluent under the flow rate of 0.28 mL/min.

S4. Spectral Data

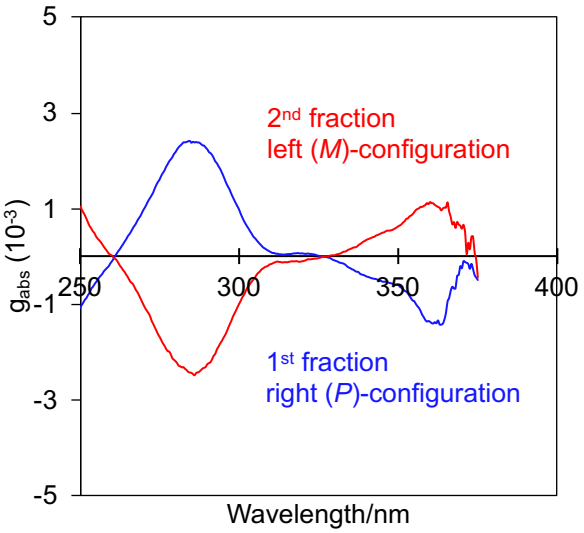

Figure S2. Plots of g_{abs} value of **C3A-1EPy** in CH_2Cl_2 solution at 25 °C (5×10^{-6} M).

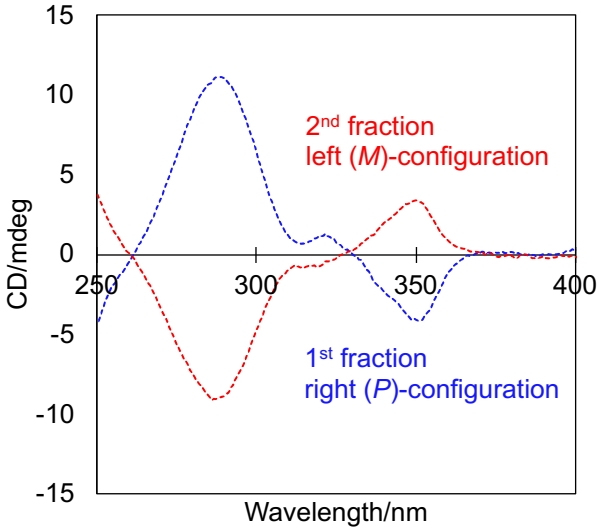

Figure S3. CD spectra of **C3A-1EPy** in CH_2Cl_2 solution at -10 °C (5×10^{-6} M).

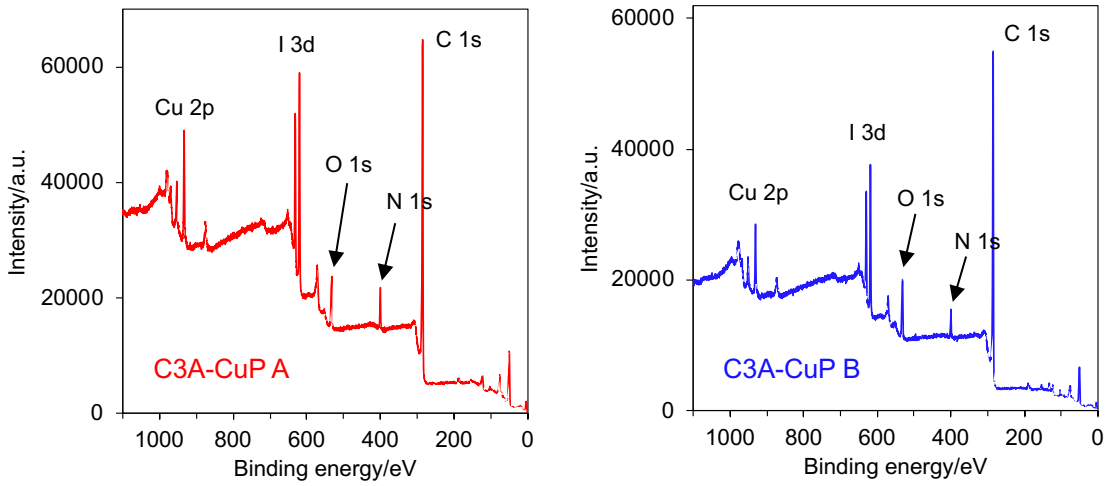

Figure S4A. Full scale XPS spectra of copper coordination polymeric complexes.

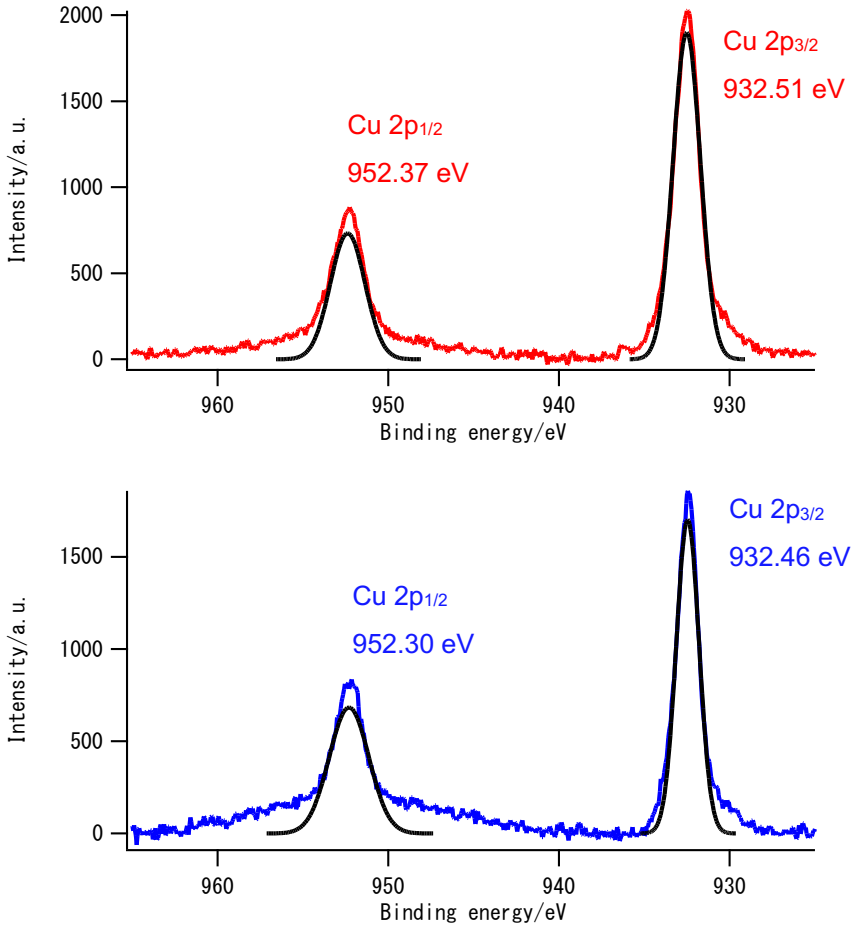

Figure S4B. Deconvoluted XPS spectra of copper coordination polymeric complexes.

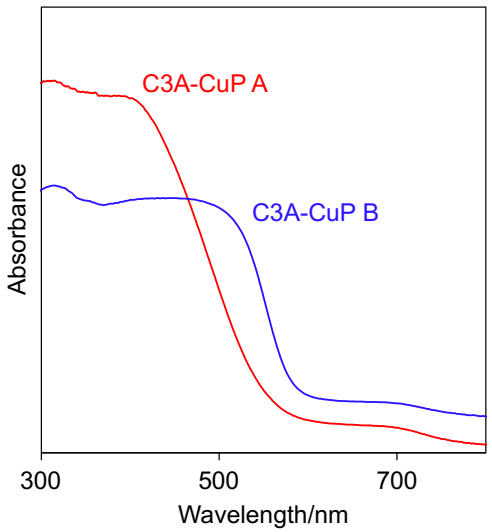

Figure S5. UV spectra of copper coordination polymeric complexes in powder state.

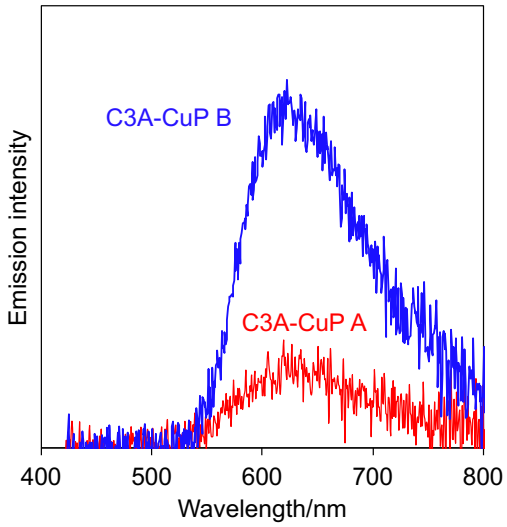

Figure S6. PL spectra of copper coordination polymeric complexes in powder state recorded on a Hamamatsu Quantaurus-QY Plus C13534 instrument under air at 25 °C, excited at 365 nm (**C3A-CuP A**) and 500 nm (**C3A-CuP B**).

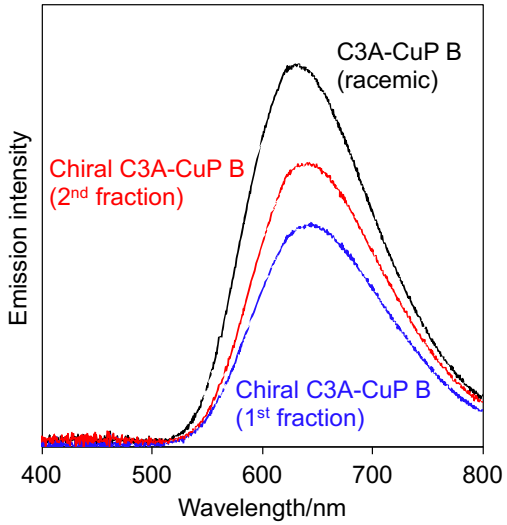

Figure S7. PL spectra of racemic (**C3A-CuP B**) and chiral (**Chiral C3A-CuP B**) copper coordination polymeric complexes in powder state under air at 25 °C, excited at 330–385 nm from a mercury lamp light source. It should be noted that the photoluminescence intensities of copper coordination polymeric complexes obtained from the chiral ligand of first and second fractions are comparable, and the difference in the intensity is due to the amount of sample measured.

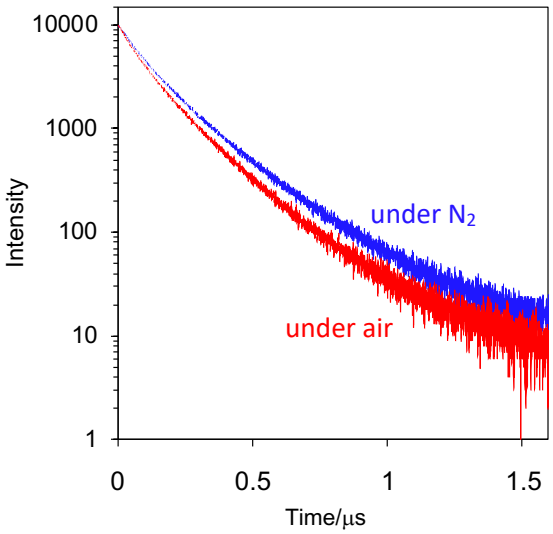

Figure S8. Photoluminescence decay curves of **Chiral C3A-CuP B** (first fraction) in powder state under air and nitrogen at 25 °C, excited at 367 nm and monitored at 630 nm.

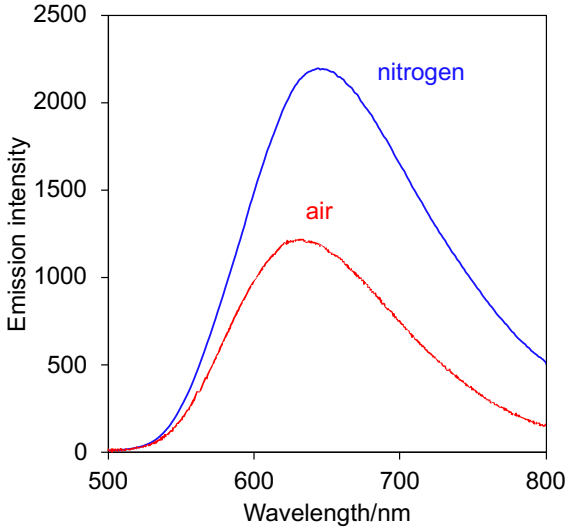

Figure S9. PL spectra of **C3A-CuP B** in powder state under air and nitrogen at 300 K, excited at 330–385 nm from a mercury lamp light source.

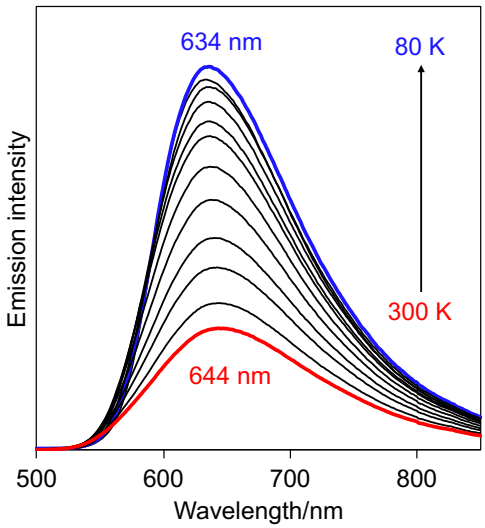

Figure S10. Variable temperature PL spectra of **Chiral C3A-CuP B** (fisrt fraction) in powder state under nitrogen from 300 K to 80 K with a 20 K interval, excited at 367 nm.

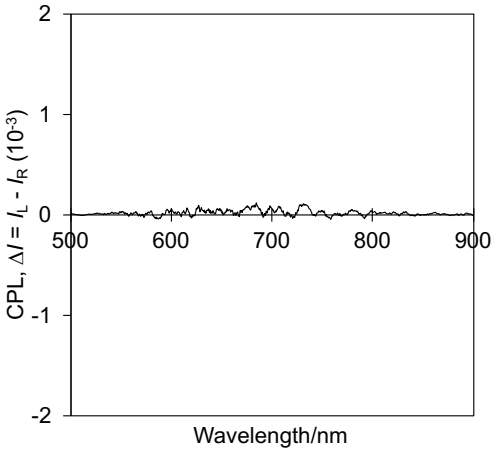

Figure S11. CPL spectra **C3A-CuP B** in the powder state under air at 25 °C, excited at 380 nm.

S5. XRD data

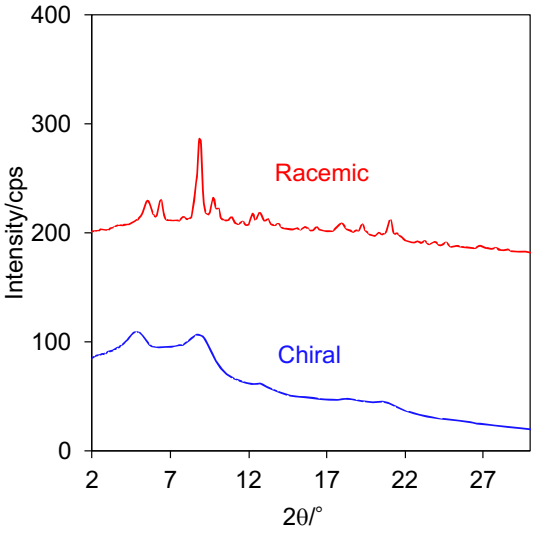

FigureS12. Powder X-ray diffraction pattern of racemic (**C3A-CuP B**) and chiral (**Chiral C3A-CuP B**) copper coordination polymeric complexes.

S6. Theoretical Calculations

DFT calculations were performed on Gaussian 09 (Revision E.01) software[S2] using computers at the Research Center for Computational Science, Okazaki, Japan. The geometries were optimized using the B3LYP and M06-2X functionals and the 6-31G(d,p) basis set. For saving the computation time, the octyl group on the amide nitrogen was replaced by the methyl group. Vibrational analyses were carried out demonstrating that all the optimized geometries correspond to energy minimum structures with no negative frequency. Theoretical UV and CD spectra were estimated by using the time-dependent DFT (TDDFT) calculation at the same level (nstates = 15).

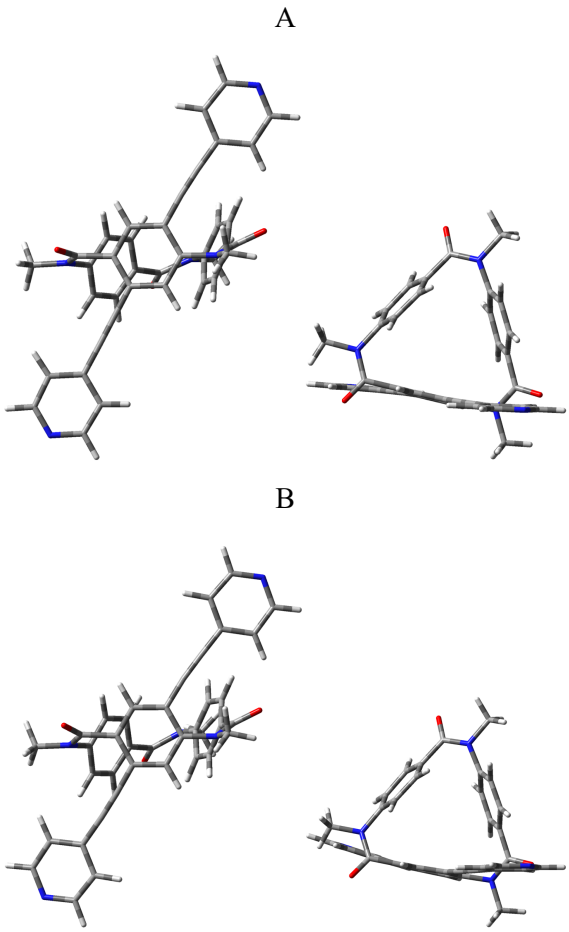

Figure S13. Tube model of optimized structures of *M*-configurational **C3A-1EPy** obtained by DTF calculation using (A) B3LYP functional and (B) M06-2X functional.

A

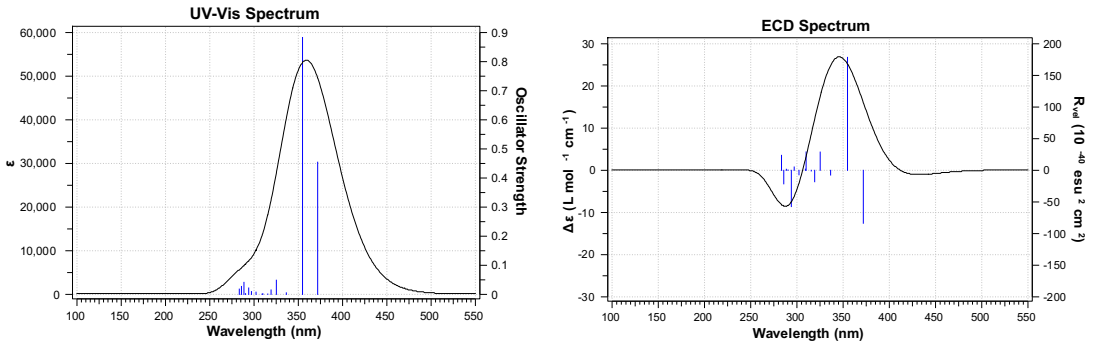

B

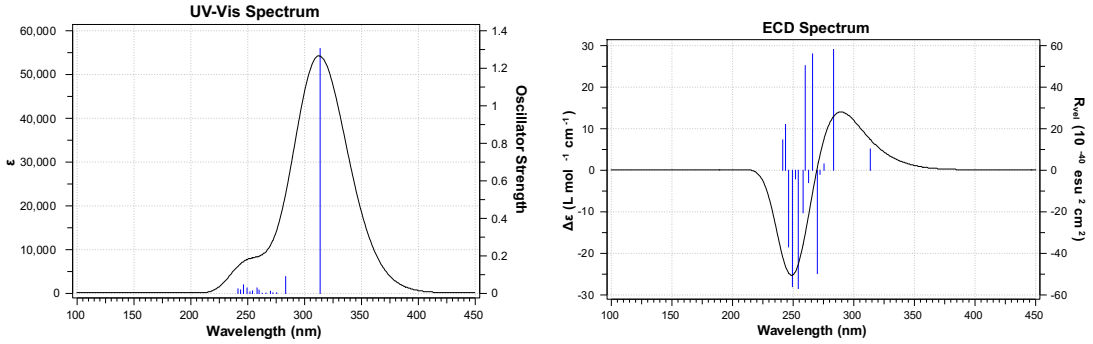

Figure S14. Theoretical UV and CD spectra of *M*-configurational **C3A-1EPy** estimated by TDDFT calculation using (A) B3LYP functional and (B) M06-2X functional. Vertical lines represent the rotatory strengths. Spectral shapes were gained by setting half width at half height at 0.333 eV.

S7. References

S1) K. Takagi, T. Shirai, D. Miyamoto, T. Nakashima, T. Ikai, Y. Ie, and T. Fukushima, *Chem. Commun.*, submitted for publication.

S2) Gaussian 09, Revision E.01, M. J. Frisch, G. W. Trucks, H. B. Schlegel, G. E. Scuseria, M. A. Robb, J. R. Cheeseman, G. Scalmani, V. Barone, B. Mennucci, G. A. Petersson, H. Nakatsuji, M. Caricato, X. Li, H. P. Hratchian, A. F. Izmaylov, J. Bloino, G. Zheng, J. L. Sonnenberg, M. Hada, M. Ehara, K. Toyota, R. Fukuda, J. Hasegawa, M. Ishida, T. Nakajima, Y. Honda, O. Kitao, H. Nakai, T. Vreven, J. A. Montgomery, Jr., J. E. Peralta, F. Ogliaro, M. Bearpark, J. J. Heyd, E. Brothers, K. N. Kudin, V. N. Staroverov, T. Keith, R. Kobayashi, J. Normand, K. Raghavachari, A. Rendell, J. C. Burant, S. S. Iyengar, J. Tomasi, M. Cossi, N. Rega, J. M. Millam, M. Klene, J. E. Knox, J. B. Cross, V. Bakken, C. Adamo, J. Jaramillo, R. Gomperts, R. E. Stratmann, O. Yazyev, A. J. Austin, R. Cammi, C. Pomelli, J. W. Ochterski, R. L. Martin, K. Morokuma, V. G. Zakrzewski, G. A. Voth, P. Salvador, J. J. Dannenberg, S. Dapprich, A. D. Daniels, O. Farkas, J. B. Foresman, J. V. Ortiz, J. Cioslowski, and D. J. Fox, Gaussian, Inc., Wallingford CT, 2013.